Теоретическая механика

Stability of Non-Linear Vibrations of Doubly Curved Shallow Shells

R. G. Mukharlyamov[*], M. Amabili[†], R. Garziera[‡], K. Riabova[‡]

[*] *Peoples Friendship University of Russia, Moscow, Russia*
[†] *McGill University, Montreal, Canada*
[‡] *University of Parma, Italy*

Large amplitude (geometrically non-linear) vibrations of doubly curved shallow shells with rectangular boundary, simply supported at the four edges and subjected to harmonic excitation normal to the surface in the spectral neighbourhood of the fundamental mode are subject of investigation in this paper. The first part of the study was presented by the authors in [M. Amabili et al. Nonlinear Vibrations of Doubly Curved Shallow Shells. Herald of Kazan Technological University, 2015, 18(6), 158–163, in Russian]. Two different non-linear strain-displacement relationships, from the Donnell's and Novozhilov's shell theories, are used to calculate the elastic strain energy. In-plane inertia and geometric imperfections are taken into account. The solution is obtained by Lagrangian approach. The non-linear equations of motion are studied by using (i) a code based on arclength continuation method that allows bifurcation analysis and (ii) direct time integration. Numerical results are compared to those available in the literature and convergence of the solution is shown. Interaction of modes having integer ratio between their natural frequencies, giving rise to internal resonances, is discussed. Shell stability under dynamic load is also investigated by using continuation method, bifurcation diagram from direct time integration and calculation of the Lyapunov exponents and Lyapunov dimension. Interesting phenomena such as (i) snap-through instability, (ii) subharmonic response, (iii) period doubling bifurcations and (iv) chaotic behavior have been observed.

Key words and phrases: nonlinear vibrations, shallow shells, equation, motion, stability

1. Introduction

In the present study [1], large-amplitude (geometrically non-linear) vibrations of doubly curved shallow shells with rectangular boundary, simply supported at the four edges and subjected to harmonic excitation normal to the surface in the spectral neighbourhood of the fundamental mode are investigated. Two different non-linear strain-displacement relationships, from the Donnell's and Novozhilov's shell theories, are used to calculate the elastic strain energy. In-plane inertia and geometric imperfections are taken into account. The solution is obtained by Lagrangian approach. The present theory is based on the studies developed by Amabili [2–4] for circular cylindrical shells, circular cylindrical panels and rectangular plates, respectively, properly adapted to take into account the different geometry. The non-linear equations of motion are studied by using (i) a code based on arclength continuation method that allows bifurcation analysis and (ii) direct time integration. The first part of the present study was published by the authors in [1]. Numerical results are compared to those available in the literature and convergence of the solution is shown. Interaction of modes having integer ratio between their natural frequencies, giving rise to internal resonances, is discussed. Shell stability under dynamic load is also investigated by using continuation method, bifurcation diagram from direct time integration and calculation of the Lyapunov exponents and Lyapunov dimension. Interesting phenomena such as (i) snap-through instability, (ii) subharmonic response, (iii) period doubling bifurcations and (iv) chaotic behavior have been observed; in this case up to four positive Lyapunov coefficients have been found, indicating hyperchaos.

2. Stability analysis

The Lagrange equations of motion for discrete models are as follows [1]:

$$\frac{\mathrm{d}q_j}{\mathrm{d}t} = \dot{q}_j, \quad \frac{\mathrm{d}q}{\mathrm{d}t}\left(\frac{\partial T_s}{\partial \dot{q}_j}\right) - \frac{\partial T}{\partial \dot{q}_j} + \frac{\partial U_s}{\partial q_j} = Q_j, \quad j = 1, \ldots, \tag{1}$$

where $\frac{\partial T}{\partial \dot{q}_j} = 0$, U_s is the elastic strain energy, the generalized coordinates q_j, $j = 1, \ldots,$ denote the displacements of an arbitrary point $A_{m,n}$ of coordinates $u_{m,n}$, $v_{m,n}$, $w_{m,n}$ in the positive directions outward the centre of the smallest radius of curvature. The very complicated term giving quadratic and cubic non-linearities can be written in the form:

$$\frac{\partial U_s}{\partial q_j} = \sum_{k=1}^{\mathrm{dofs}} q_k \tilde{z}_{j,k} + \sum_{i,k=1}^{\mathrm{dofs}} q_i q_k \tilde{z}_{j,i,k} + \sum_{i,k,i=1}^{\mathrm{dofs}} q_i q_k q_l \tilde{z}_{j,i,k,l}, \tag{2}$$

where coefficients $\tilde{z}$ have long expressions that include also geometric imperfections.

The presumable solution of the system (1) is $q_j = q_j(t)$, $\dot{q}_j = \dot{q}_j(t)$, which corresponds to an undisturbed motion. After defining the excitations of the phase coordinates of the system as $x_j = q_j - q_j(t)$, $y_j = \dot{q}_j - \dot{q}_j(t)$, the equations of the perturbed motions can be presented in the frame of the first approximation:

$$\begin{cases} \dfrac{\mathrm{d}x_j}{\mathrm{d}t} = y_j, \\ \dfrac{\mathrm{d}y_j}{\mathrm{d}t} = -\displaystyle\sum_{i=1}^{\mathrm{dofs}} a_{ji} x_i - \sum_{i=1}^{\mathrm{dofs}} b_{ji} y_i - \sum_{i=1}^{\mathrm{dofs}} c_{jn} x_n, \quad a_{ji} = z_{ji}, \quad b_{ji} = 2\varsigma_j \omega_j, \end{cases} \tag{3}$$

$$c_{jn}(t) = \sum_{i=1}^{\mathrm{dofs}} z_{jin} q_i(t) + \sum_{k=1}^{\mathrm{dofs}} z_{jnk} q_k(t) + \sum_{k=1}^{\mathrm{dofs}}\sum_{l}^{\mathrm{dofs}} z_{jnkl} q_k(t) q_l(t) +$$

$$+ \sum_{i=1}^{\mathrm{dofs}}\sum_{1}^{\mathrm{dofs}} z_{jinl} q_i(t) q_l(t) + \sum_{i=1}^{\mathrm{dofs}}\sum_{k}^{\mathrm{dofs}} z_{jikn} q_i(t) q_k(t).$$

If the conditions

$$z_{jin} = 0, \quad z_{jnk} = 0, \quad z_{jnkl} = 0, \quad z_{jinl} = 0, \quad z_{jikn} = 0,$$
$$i = 1, \ldots, \mathrm{dofs}, \quad j = 1, \ldots, \mathrm{dofs}, \quad k = 1, \ldots, \mathrm{dofs} \tag{4}$$

are satisfied the system of equations of the perturbed motions becomes a system of linear differential equations with constant coefficients

$$\begin{cases} \dfrac{\mathrm{d}x_j}{\mathrm{d}t} = y_j, \\ \dfrac{\mathrm{d}y_j}{\mathrm{d}t} = -\displaystyle\sum_{i=1}^{\mathrm{dofs}} a_{ji} x_i - \sum_{i=1}^{\mathrm{dofs}} b_{ji} y_i. \end{cases} \tag{5}$$

In this case the stability of the solution of the system (1) can be analyzed by means of the characteristic equation

$$\det(A - \lambda E) = 0 \tag{6}$$

of the system (5), where $A = \begin{bmatrix} 0 & \delta_{ji} \\ -a_{ji} & -b_{ji} \end{bmatrix}$.

Once all the roots of the characteristic equation (6) have negative real parts, then the trivial solution $x_j = 0$, $y_j = 0$ of the system (5) is asymptotically stable.

In this case there exists a Lyapunov's function of fixed sign $V = V(x, y)$, and its derivative, which can be obtained from the equations (3), is also a function of fixed sign of the opposite sign. This means that the solutions of the initial system $q_j(t)$, $\dot{q}_j = \dot{q}_j(t)$ for which the conditions (4) are valid, result as asymptotically stable.

The variable-coefficient system (3) can be written in the matrix formulation as follows:

$$\frac{\mathrm{d}\tilde{x}}{\mathrm{d}t} = B(t)\tilde{x}, \quad \tilde{x} = (x_1, \cdots, x_j, y_1, \cdots, y_j), \tag{7}$$

$$D = \begin{bmatrix} 0 & D \\ -A - C(t) & -B \end{bmatrix}, \ D = (\delta_{ji}), \ A = (a_{ji}), \ C(t) = \big(\delta_{jn}c_{jn}(t)\big), \ B = (b_{ji}). \tag{8}$$

The Lyapunov's function can be written as a quadratic form with constant coefficients

$$2V = \tilde{x}^T M \tilde{x}, \tag{9}$$

where $\tilde{x} = (x, y)$ and $M = \begin{bmatrix} M_{11} & M_{12} \\ M_{21} & M_{22} \end{bmatrix}$.

The derivative of V calculated from the equation (7) can be presented in the following form:

$$\dot{V} = W(x, y) - K(x, y, t), \tag{10}$$

$$W(x, y) = -x^T M_{12} A x - y^T M_{22} A x + x^T (M_{11} D - M_{12} B) y + y^T (M_{12} D - M_{22} B) y, \tag{11}$$

$$K(x, y, t) = (x^T M_{12} + y^T M_{22}) C(t) x. \tag{12}$$

From the expression (10) for $\dot{V}$ the following conclusion can be drawn: if the quadratic form $W(x, y)$ is a function of fixed negative sign, then the solutions $q_j = q_j(t)$, $\dot{q}_j = \dot{q}_j(t)$ of the system (1) for which $K(x, y, t) \equiv 0$ are asymptotically stable.

3. Numerical solution

The equations of motion have been obtained by using the Mathematica 4 computer software [5] in order to perform analytical integrals of trigonometric functions. The generic Lagrange equation can be divided by the modal mass associated with $\ddot{q}_j$ and then is transformed in the following two first-order equations by using the dummy variables y_j in a similar way as shown in the previous section

$$\begin{cases} \dot{q}_j = y_j, \\ \dot{y}_j = -2\varsigma_j \omega_j y_j - \sum_{i=1}^{\text{dofs}} z_{j,i} q_i - \sum_{i=1}^{\text{dofs}}\sum_{k=1}^{\text{dofs}} z_{j,i,k} q_i q_k - \sum_{i=1}^{\text{dofs}}\sum_{k=1}^{\text{dofs}}\sum_{l=1}^{\text{dofs}} q_i q_k q_l + f \cos(\omega t) \end{cases} \tag{13}$$

for $j = 1, \ldots, \text{dofs}$, where

$$f = \begin{cases} 0, & \text{if } q_j = u_{m,n}, \ v_{m,n}, \ \text{or } w_{m,n} \text{ with } m, n \text{ even}, \\ \tilde{f}/[\rho_s hab/4], & \text{if } q_j = w_{m,n} \text{ with } m, n \text{ odd}, \end{cases}$$

$\tilde{f}$ is the radial concentrated force, which define the external, normal, distributed load such that $q_w = \tilde{f}\delta(u - \tilde{u})\cos(\omega t)$, applied to the shell, $\tilde{u}$, $\tilde{v}$ give the position of the point of application of the force; the point excitation is located at $\tilde{u} = a/2$, $\tilde{v} = b/2$, ω is the excitation frequency, t is the time, δ is the Dirac delta function, and coefficients z are obtained by those in equation (2), $z = \tilde{z}/[\rho_s hab/4]$.

In equation (13) each generalized coordinate q_j (and therefore $\varsigma - j$ and ω_j) has to be referred to mode (m, n). A non-dimensionalization of variables is also performed for computational convenience: the time is divided by the period of the resonant mode and the vibration amplitudes are divided by the shell thickness h. The resulting $2 \times$ dofs first-order non-linear differential equations are studied by using (i) the software AUTO 97 [6] for continuation and bifurcation analysis of non-linear ordinary differential equations, and (ii) direct integration of the equations of motion by using the DIVPAG routine of the Fortran library IMSL. Continuation methods allow following the solution path, with the advantage that unstable solutions can also be obtained; these are not ordinarily attainable by using direct numerical integration. The software AUTO 97 is capable of continuation of the solution, bifurcation analysis and branch switching by using arclength continuation and collocation methods. In particular, the shell response under harmonic excitation has been studied by using an analysis in two steps: (i) first the excitation frequency has been fixed far enough from resonance and the magnitude of the excitation has been used as bifurcation parameter; the solution has been started at zero force where the solution is the trivial undisturbed configuration of the shell and has been continued up to reach the desired force magnitude; (ii) when the desired magnitude of excitation has been reached, the solution has been continued by using the excitation frequency as bifurcation parameter.

Direct integration of the equations of motion by using Gear's BDF method (routine DIVPAG of the Fortran library IMSL) has also been performed to check the results and obtain the time behaviour. Adams Gear algorithm has been used due to the relatively high dimension of the dynamical system. Indeed, when a high-dimensional phase space is analyzed, the problem can present stiff characteristics, due to the presence of different time scales in the response. In simulations with adaptive step size Runge-Kutta methods, spurious non-stationary and divergent motions can be obtained. Therefore, the Adams Gear method, designed for stiff equations, was used.

The bifurcation diagram of the Poincaré maps was also used in case of non-stationary response. It has been constructed by using the time integration scheme and by varying the force amplitude.

3.1.   Maximum Lyapunov exponent

In order to evaluate the maximum Lyapunov exponent, which is useful to characterize regular or chaotic motion of the system, it is necessary to assume a reference trajectory $x_r(t)$ in the phase plane $(q, \dot{q}$ plane) and observe a neighbouring trajectory originated at infinitesimal initial perturbation $\delta x(t_0)$ from the reference trajectory (see Argyris et al. [7]). The evolution of the perturbation during time, $\delta x(t)$, is governed by the following variational equations directly obtained from equations (13)

$$\frac{\mathrm{d}}{\mathrm{d}t}\delta q_j = \delta y_j,$$

$$\frac{\mathrm{d}}{\mathrm{d}t}\delta y_j = -2\varsigma_j\varpi_j\delta y_j - \sum_{i=1}^{\mathrm{dofs}} z_{j,i}\delta q_i - \sum_{n=1}^{\mathrm{dofs}}\sum_{i=1}^{\mathrm{dofs}}\sum_{k=1}^{\mathrm{dofs}} z_{j,i,k}\delta q_n(\delta_{k,n}q_i + \delta_{i,n}q_k)-$$

$$-\sum_{n=1}^{\text{dofs}}\sum_{i=1}^{\text{dofs}}\sum_{k=1}^{\text{dofs}}\sum_{l=1}^{\text{dofs}} z_{j,i,k,l}\delta q_n(\delta_{i,n}q_kq_l + \delta_{k,n}q_iq_l + \delta_{l,n}q_kq_i), \text{ for } j=1,\dots,\text{dofs}, \quad (14)$$

where $\delta_{k,n}$ is the Kronecker delta. Assuming δq_j and δy_j as new variables, the simultaneous integration of the $4 \times$ dofs first-order differential equations (equations (13) are non-linear and are integrated by using DIVPAG IMSL routine and equations (14) are linear, but with time-varying coefficients, and are integrated by using the adaptive step-size 4th-5th order Runge-Kutta method) has been performed. The excitation period has been divided in 10000 integration steps Δt in order to have accurate evaluation of the time-varying coefficients in equations (14) that are obtained at each step by integration of equations (13). To find a reference trajectory 6×10^6 steps are waited in order to eliminate the transitory and 1×10^6 steps are waited to eliminate the transitory on the variational equations (14). Then 1×10^6 steps are used for evaluation of the maximum Lyapunov exponent σ_1 for the reference trajectory $x_r(t)$, which is given by

$$\sigma_1 = \lim_{t\to\infty} \sup \frac{1}{t}\ln\frac{|\delta x(t)|}{|\delta x(t_0)|}. \quad (15)$$

Assuming the initial perturbation of unitary amplitude, equation (15) is simplified into

$$\sigma_1 = \lim_{t\to\infty} \sup \frac{1}{t}\ln|\delta x(t)|. \quad (16)$$

Then, by restoring at each integration time step k the amplitude of $\delta x(t)$ to its original unitary measure by the following re-normalisation

$$\delta\overline{x}(t)_k = \frac{\delta x(t)_k}{d_k}, \quad (17)$$

where $|\delta x(t)|_k = d_k$, the following formula for the maximum Lyapunov exponent, evaluated at step k, is obtained

$$\sigma_{1,k} = \frac{1}{k\Delta t}\sum_{i=1}^{k}\ln d_i. \quad (18)$$

In the numerical calculation of the maximum Lyapunov exponent, the non-dimensional time previously introduced has been used.

4.   Results for harmonic excitation

Numerical calculations have been initially performed for doubly curved shallow shells, simply supported at the four edges, having the following dimensions and material properties: curvilinear dimensions $a = b = 0.1m$, radius of curvature $R_x = 1m$, thickness $h = 0.001m$, Young's modulus $E = 206 \times 10^9$ Pa, mass density $\rho = 7800$ kg/m^3 and Poisson ratio $\nu = 0.3$. Shallow shells with the same dimension ratios ($R_x/a = 10$, $h/a = 0.01$, $a/b = 1$, $\nu = 0.3$) were previously studied by Kobayashi and Leissa [8]. In all the numerical simulations a modal damping $\varsigma_{1,1} = 0.004$ and harmonic force excitation at the center of the shell in z direction are assumed. If not explicitly specified, all calculations have been performed by using Donnell's shell theory.

4.1. Case of a spherical shell

A spherical shallow shell ($R_y = 1m$) is considered. The frequency range around the fundamental frequency (mode ($m = 1$, $n = 1$) in this case, where m and n are the numbers of half-waves in x and y direction, respectively) is investigated. The fundamental frequency $\omega_{1,1}$ is 952.31 Hz according to Donnell's shell theory and 952.26 Hz according to Novozhilov's shell theory, i.e. practically the same results for both theories. Other natural frequencies useful in the present study are (according to Donnell's theory): $\omega_{1,3} = \omega_{3,1} = 2575.9$ Hz, $\omega_{3,3} = 4472.3$ Hz. The amplitude of the harmonic force is $\widetilde{f} = 31.2$ N.

Figure 1 shows the maximum (in the time period; this is positive, i.e. outwards) and the minimum (negative, i.e. inwards) of the shell response in z direction in the spectral neighbourhood of the fundamental mode ($m = 1$, $n = 1$) versus the excitation frequency.
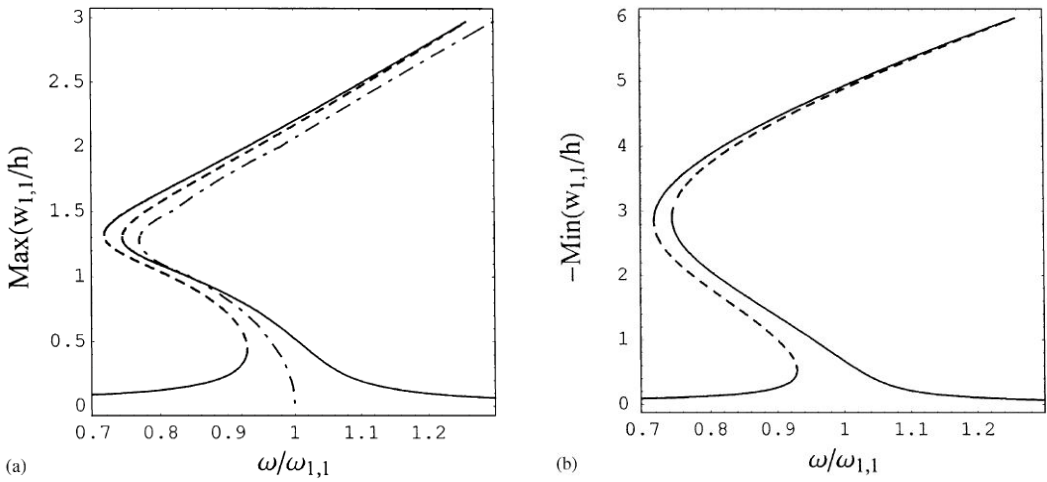

Figure 1. Amplitude of the response of the shell (generalized coordinate $w_{1,1}$) versus the excitation frequency; $R_x/R_y = 1$ (spherical shallow shell); fundamental mode ($m = 1$, $n = 1$), $\widetilde{f} = 31.2$ N and $\zeta_{1,1} = 0.004$; model with 9 dofs; Donnell's theory: solid line —— present stable results; dashed line — present unstable results; dot-dashed line — backbone curve from Kobayashi and Leissa [8]. (a) Maximum of the generalized coordinate $w_{1,1}$ (in a vibration period); (b) minimum of the generalized coordinate $w_{1,1}$

Calculations have been performed with the 9 dofs model. This model includes the following terms in the expressions for displacements u, v and w, which satisfy identically the geometric boundary conditions [1]: $w_{1,1}$, $u_{1,1}$, $v_{1,1}$, $u_{3,1}$, $v_{3,1}$, $u_{1,3}$, $v_{1,3}$, $u_{3,3}$, $v_{3,3}$.

Results are compared to those obtained by Kobayashi and Leissa [8], where only the backbone curve is given. The present results with 9 dofs are quite close to those in references [8] (considering that the backbone curve, indicating the maximum of the response for different force excitations, approximately passes through the middle of the forced response curve computed in the present calculation) and shows a softening type non-linearity, turning to hardening for vibration amplitudes about two times larger than the shell thickness. Comparing Figures 1,(a) and 1,(b) it is evident that displacement inwards is about two times larger than displacement outwards during a vibration period.

In order to check the convergence of the solution, the response has been calculated with a larger model, including 22 dofs. This model has the following additional generalized coordinates with respect to the 9 dofs model: $w_{1,3}$, $w_{3,1}$, $w_{3,3}$, $u_{1,5}$, $u_{3,5}$, $u_{5,1}$, $u_{5,3}$, $u_{5,5}$, $v_{1,5}$, $v_{3,5}$, $v_{5,1}$, $v_{5,3}$, $v_{5,5}$.

Comparison of the response computed with the 22 dofs and the 9 dofs models is given in Figure 3, where the backbone curve of Kobayashi and Leissa [8] is also shown.

The results of the 22 dofs model are moved slightly to the left with respect to the smaller 9 dofs model, and present a more complicate curve, especially in the frequency region around $0.9\omega_{1,1}$. In fact, for excitation frequency $\omega = 0.9\omega_{1,1}$, there is a 3:1 internal resonance with modes $(m = 3, n = 1)$ and $(m = 1, n = 3)$, giving $3\omega = \omega_{3,1} = \omega_{1,3}$. A second relationship between natural frequencies that leads to internal resonances is for $\omega = 0.77\omega_{1,1}$ where $6\omega = \omega_{3,3}$.
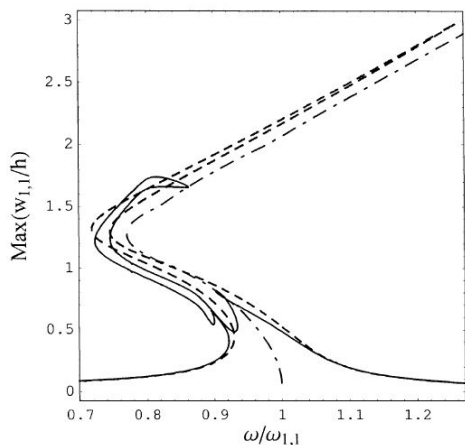

Figure 2. Amplitude of the response of the shell versus the excitation frequency; $R_x/R_y = 1$ (spherical shell); fundamental mode ($m = 1$, $n = 1$), $\tilde{f} = 31.2$ N and $\zeta_{1,1}\zeta_{1,1} = 0.004$; Donnell's theory: solid line —— 22 dofs model; dashed line — 9 dofs model; dot-dashed line — backbone curve from Kobayashi and Leissa [8]
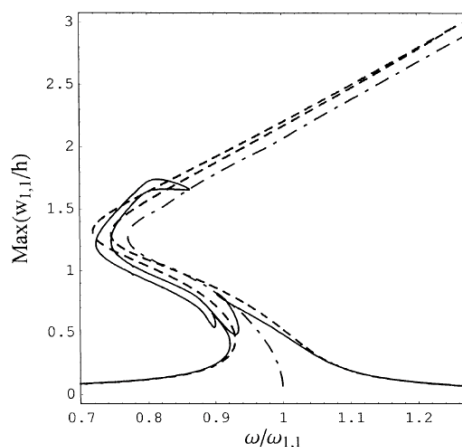
Figure 3. Effect of the curvature aspect ratio R_x/R_y on the shell response (maximum of the generalized coordinate $w_{1,1}$) versus the excitation frequency; fundamental mode ($m = 1$, $n = 1$); $\zeta_{1,1} = 0.004$; 9 dofs model; Donnell's theory

4.2. Effect of different curvature

Figure 3 synthesizes all the maximum responses for the 9 dofs model for different shell curvature aspect ratios R_x/R_y. It is clearly shown that for $R_x/R_y = 1$ (spherical), 0.5 and 0 (circular cylindrical) the shallow shell considered exhibits a softening type behaviour turning to hardening type for vibration amplitude of the order of magnitude of the shell thickness. The softening behaviour becomes weaker with the decrement of the curvature aspect ratio R_x/R_y. In particular, the softening behaviour of the spherical shallow shell for vibration amplitude around 1.3 times the shell thickness is very strong. On the other hand, for $R_x/R_y = -0.5, -1$ (hyperbolic paraboloid) the shell has a strong hardening type behaviour without presence of the softening type region.

The effect of the curvature on the maximum response of spherical shallow shells is investigated in Figure 4, obtained with the 9 dofs model and Donnell's shell theory. Here the radius of curvature $R_x = R_y$ is varied with respect to the value $1m$ previously used, while all the other geometric and material characteristics are kept constant. In particular, three responses for $R_x/a = 10, 20, 100$ are presented (solid line) and compared to the response of a flat square plate (dashed line) of the same dimension and material, also computed with the same theory [4] and the 9 dofs model. It must be observed that the

flat plate is the limiting case for a spherical shallow shell when $R_x/a \to \infty$. Figure 4 shows that increasing the curvature ratio R_x/a the shell response changes gradually from (i) strongly softening turning to hardening for vibration amplitude about two times the shell thickness, to (ii) fully hardening, which is the typical behaviour of flat plates. It is curious that a flat plate ($R_x/a \to \infty$) presents a slightly weaker hardening type behaviour than the spherical shallow shell with $R_x/a = 100$. However, the difference is practically negligible.
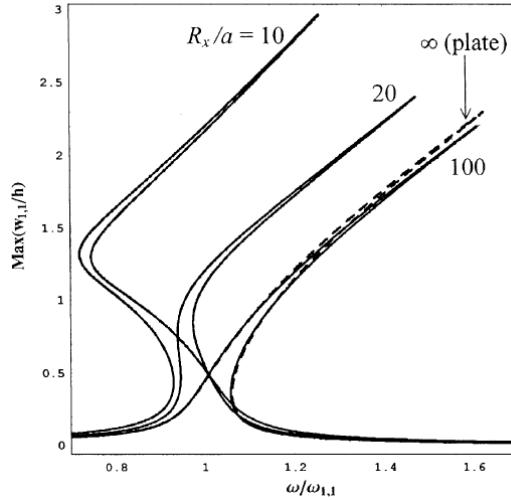

Figure 4. Effect of the curvature ratio R_x/a on the response (maximum of the generalized coordinate $w_{1,1}$) of spherical shallow shells versus the excitation frequency; fundamental mode ($m = 1$, $n = 1$); $\zeta_{1,1} = 0.004$; 9 dofs model; Donnell's theory. For $R_x/a = 10$, $w_{1,1} = 952.3$ Hz and $\widetilde{f} = 31.2$ N; for $R_x/a = 20$, $w_{1,1} = 637.1$ Hz and $\widetilde{f} = 11.16$ N; for $R_x/a = 100$, $w_{1,1} = 495.4$ Hz and $\widetilde{f} = 5.56$ N; for $R_x/a = \infty$ (square plate), $w_{1,1} = 488.6$ Hz and $\widetilde{f} = 5.4$ N

5.   Bifurcation analysis

The same shallow spherical shell studied in Section 4.1 is considered here and the 22 dofs model is used. Poincaré maps have been computed by direct integration of the equations of motion. The excitation frequency has been kept constant, $\omega = 0.8\omega_{1,1}$, and the excitation amplitude has been varied between 0 and 1400 N. The force range has been divided into 800 steps, so that the force is varied of 1.75 N at each step. 600 periods have been waited each time the force is changed of a step in order to eliminate the transient motion. The initial condition at the first step is zero displacement and velocity for all the variables; at the following steps the solution at the previous step, with addition of a small perturbation in order to find stable solution, is used as initial condition. The bifurcation diagrams obtained by all these Poincaré maps are shown in Figure 5, where the load is decreased from 1400 N to 0.

Simple periodic motion, period doubling bifurcation, subharmonic response, amplitude modulations and chaotic response have been detected, as indicated in Figures 5,(a), 5,(b). This indicates a very rich and complex nonlinear dynamics of the spherical shallow shell subject to large harmonic excitation. Different stable solutions coexist for the same set of system parameters, so that the solution is largely affected by initial conditions. In particular, Figures 5,(b) and 5,(d) give the maximum Lyapunov exponent σ associated

to the bifurcation diagram. It can be easily observed that (i) for periodic forced vibrations $\sigma_1 < 0$, (ii) for amplitude modulated response $\sigma_1 = 0$, and (iii) for chaotic response $\sigma_1 > 0$. Therefore σ can be conveniently used for identification of the system dynamics.
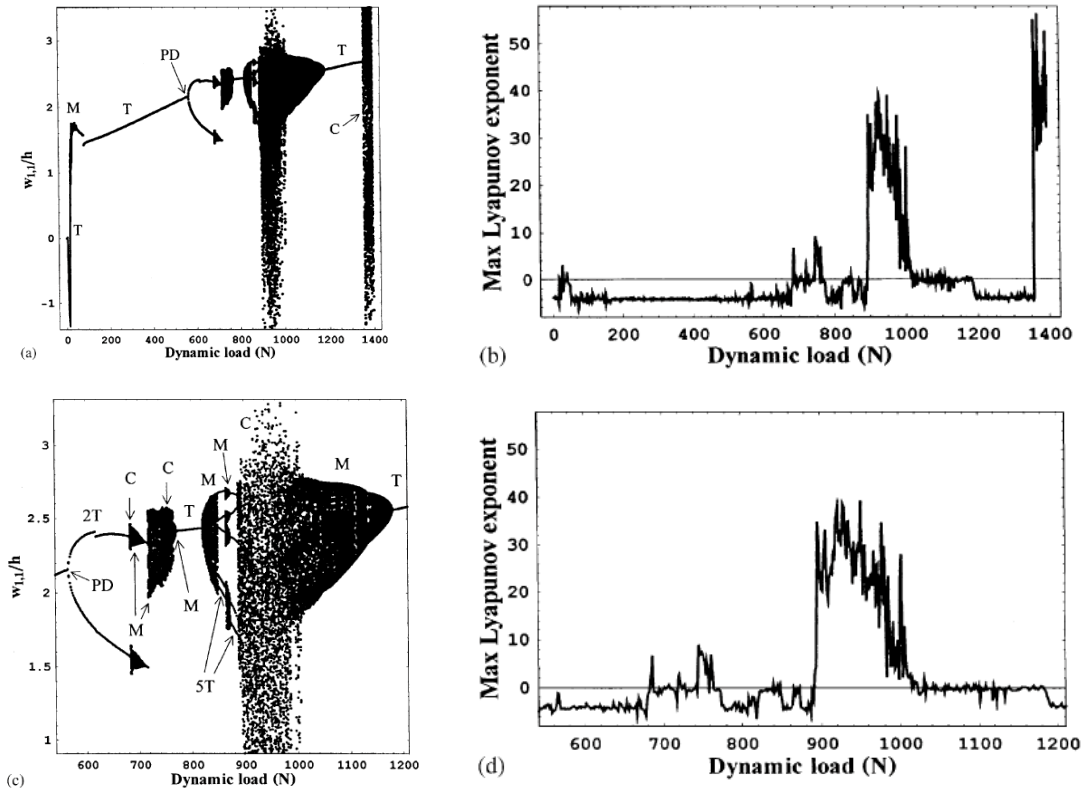

Figure 5. Bifurcation diagram of Poincaré maps and maximum Lyapunov exponent for the spherical shallow shell under decreasing harmonic load with frequency $\omega = 0.8\omega_{1,1}$; $\zeta_{1,1} = 0.004$; 22 dofs model; Donnell's theory:
(a) Bifurcation diagram: generalized coordinate $w_{1,1}$; T =response period equal to excitation period; PD =period doubling bifurcation; M =amplitude modulations; C =chaos;
(b) maximum Lyapunov exponent;
(c) bifurcation diagram: generalized coordinate $w_{1,1}$, enlarged scale; T =response period equal to excitation period; PD =period doubling bifurcation; $2T$ =periodic response with two times the excitation period; $5T$ =periodic response with five times the excitation period; M =amplitude modulations; C =chaos;
(d) maximum Lyapunov exponent, enlarged scale

All the Lyapunov exponents have been evaluated for the case with excitation $\widetilde{f} =$ 1396 N in Figure 5, corresponding to chaotic response. In this case, four positive Lyapunov exponents have been identified, allowing to classify this response as hyperchaos. The Lyapunov dimension in this case is $d_L = 24.59$.

6.   Conclusions

The present study introduces a multi-mode expansion and uses accurate shell theories retaining in-plane inertia to study large-amplitude, forced vibrations of doubly curved shallow shells. This overcomes two frequent limitations in previous studies: (i) the use of mode expansions with one or two degrees of freedom; and (ii) the use of less accurate, but simpler, Donnell's shallow-shell theory, which neglects in-plane inertia. The occurrence of internal resonances in the problem studied is a clear indication that this important non-linear phenomenon has fundamental importance in the study of curved shells. Internal resonances can be studied only with multi-mode expansions, in some cases with a quite large number of degrees of freedom.

Bifurcation diagrams constructed by Poincaré maps and Lyapunov exponents show period doubling bifurcations and highly complex nonlinear behaviour of a spherical shallow shell under very large harmonic excitation. Up to four positive Lyapunov coefficients have been found for the studied case, indicating hyperchaos.

References

1. M. Amabili, R. Garziera, R. Mukharlyamov, K. Riabova, Nonlinear Vibrations of Doubly Curved Shallow Shells, Herald of Kazan Technological University 18 (6) (2015) 158–163, in Russian.
2. M. Amabili, Comparison of Shell Theories for Large-Amplitude Vibrations of Circular Cylindrical Shells: Lagrangian Approach, Journal of Sound and Vibration (264) (2003) 1091–1125.
3. M. Amabili, Nonlinear Vibrations of Circular Cylindrical Panels, Journal of Sound and Vibration (281) (2005) 509–535.
4. M. Amabili, Nonlinear Vibrations of Rectangular Plates with Different Boundary Conditions: Theory and Experiments, Computers and Structures (82) (2004) 2587–2605.
5. S. Wolfram, The Mathematica Book, 4th edition, Cambridge, UK: Cambridge University Press, 1999.
6. E. J. Doedel, A. R. Champneys, T. F. Fairgrieve, Y. A. Kuznetsov, B. Sandstede, X. Wang, AUTO 97: Continuation and Bifurcation Software for Ordinary Differential Equations (with HomCont), Montreal, Canada: Concordia University, 1998.
7. J. Argyris, G. Faust, M. Haase, An Exploration of Chaos, Amsterdam: North-Holland, 1994.
8. Y. Kobayashi, A. W. Leissa, Large Amplitude Free Vibration of Thick Shallow Shells Supported by Shear Diaphragms, International Journal of Non-Linear Mechanics (30) (1995) 57–66.

Устойчивость нелинейных колебаний пологих оболочек двоякой кривизны

Р. Г. Мухарлямов[*], **М. Амабили**[†], **Р. Гарзиера**[‡], **К. Рябова**[‡]

[*] *Российский университет дружбы народов, Москва, Россия*
[†] *Университет МакГилл, Монреаль, Канада*
[‡] *Университет Пармы, Парма, Италия*

В статье рассматриваются высокоамплитудные (геометрически нелинейные) колебания пологих оболочек двоякой кривизны с прямоугольными границами, свободно опертых по всем четырем краям и подвергающихся нормальному к поверхности гармоническому воздействию в спектральной окрестности основной формы. Первая часть проведенных исследований была представлена в работе [М. Амабили и др. Нелинейные колебания пологих

оболочек двоякой кривизны // Вестник КГТУ, 2015. — Т. 18, № 6. — С. 158–163] авторов. Для расчета энергии упругой деформации были использованы два различных нелинейных соотношения между деформацией и перемещением: из теории Доннелла и теории Новожилова. Учитывались также геометрические несовершенства формы оболочкии и влияние инерции в плоскости. Построены приближенные уравнения динамики в форме уравнений Лагранжа второго рода. Предполагается, что потенциальная энергия сил упругости разлагается в ряд, в котором ограничиваются членами третьего порядка. Для исследования устойчивости невозмущенного движения используется метод функций Ляпунова и метод характеристичных чисел. Полагая функцию Ляпунова квадратичной формой с постоянными коэффициентами, определяются условия, при которых решение, соответствующее невозмущенному движению системы при гармоническом воздействии, является устойчивым. Определяется оценка наибольшего характеристичного числа Ляпунова. Приводятся результаты численных экспериментов, полученных для системы с гармоническим возбуждением. Рассматривается случай сферической оболочки, исследуется эффект влияния различной кривизны, проводится бифуркационный анализ.

Ключевые слова: нелинейные колебания, пологие оболочки, уравнение, движение, устойчивость

Литература

1. Нелинейные колебания пологих оболочек двоякой кривизны / М. Амабили, Р. Гарзиера, Р. Мухарлямов, К. Рябова // Вестник КГТУ. — 2015. — Т. 18, № 6. — С. 158–163.

2. *Amabili M.* Comparison of Shell Theories for Large-Amplitude Vibrations of Circular Cylindrical Shells: Lagrangian Approach // Journal of Sound and Vibration. — 2003. — No 264. — Pp. 1091–1125.

3. *Amabili M.* Nonlinear Vibrations of Circular Cylindrical Panels // Journal of Sound and Vibration. — 2005. — No 281. — Pp. 509–535.

4. *Amabili M.* Nonlinear Vibrations of Rectangular Plates with Different Boundary Conditions: Theory and Experiments // Computers and Structures. — 2004. — No 82. — Pp. 2587–2605.

5. *Wolfram S.* The Mathematica Book, 4th edition. — Cambridge, UK: Cambridge University Press, 1999.

6. AUTO 97: Continuation and Bifurcation Software for Ordinary Differential Equations (with HomCont) / E. J. Doedel, A. R. Champneys, T. F. Fairgrieve, Y. A. Kuznetsov, B. Sandstede, X. Wang. — Montreal, Canada: Concordia University, 1998.

7. *Argyris J., Faust G., Haase M.* An Exploration of Chaos. — Amsterdam: North-Holland, 1994.

8. *Kobayashi Y., Leissa A. W.* Large Amplitude Free Vibration of Thick Shallow Shells Supported by Shear Diaphragms // International Journal of Non-Linear Mechanics. — 1995. — No 30. — Pp. 57–66.